Engineering Science and Technology, an International Journal 19 (2016) 90–95

HOSTED BY

Contents lists available at ScienceDirect

Engineering Science and Technology, an International Journal

journal homepage: http://www.elsevier.com/locate/jestch

Full Length Article

Investigation of interdiffusion and intermetallic compounds in Al–Cu joint produced by continuous drive friction welding

Yanni Wei [a,b], Jinglong Li [b,*], Jiangtao Xiong [a,b], Fusheng Zhang [b]

[a] State Key Laboratory of Solidification Processing, Northwestern Polytechnical University, Xi'an 710072, China
[b] Shaanxi Key Laboratory of Friction Welding Technologies, Northwestern Polytechnical University, Xi'an 710072, China

ARTICLE INFO

Article history:
Received 27 November 2014
Received in revised form
27 May 2015
Accepted 27 May 2015
Available online 13 August 2015

Keywords:
Continuous drive friction welding
Formation Gibbs free energy
Intermetallic phase
Interdiffusion
Al–Cu joint

ABSTRACT

In this paper, the joints between Al and Cu bars were fabricated by continuous drive friction welding. The microstructures and the compositions of the composites were analyzed by SEM, EDS and XRD. The surface temperature was observed using an infrared thermographic camera. The interface temperatures were suggested in the range of 648~723 K at different welding parameters. The interdiffusion between Al and Cu atoms is extraordinarily rapid, as the interdiffusion coefficients could reach 7.8×10^{-12} m^2/s. Intermetallic phases Al_2Cu and Al_4Cu_9 were identified in all samples in view of the XRD and EDS analyses. The effective Gibbs free energy change of formation model was proposed to predict the Al–Cu compound formation at solid-state interface, and the calculation combined with kinetic factors showed that Al_2Cu (Al side) and Al_4Cu_9 (Cu side) appeared first.

1. Introduction

The ratio of conductivity to density is about two times greater for Al relative to Cu. It would be attractive to replace certain Cu parts of power transmission systems with Al when weight and cost are design considerations [1,2]. Therefore, the joining of dissimilar materials of Al and Cu should allow a more optimized design solution for power transmission systems. Al and Cu are incompatible metal because they have a high affinity to each other at temperature greater than 120 °C and produce several kinds of intermetallics on their interface [3,4]. These brittle intermetallic phases have significant influence on the manufacturability, mechanical properties, and reliability of the Al–Cu structures [5,6]. Therefore, to understand the interdiffusion and intermetallic phase formation at the Al–Cu interface is of both scientific and technological importance.

The interdiffusion between Al and Cu is accompanied by the intermetallic formation, and the interdiffusion coefficients of Al and Cu in each of these formations are dissimilar [7]. Then the width of the diffusion layer is related with not only diffusion time but also the amount of each of the formations. Du et al. [8] studied the diffusion of Cu in face-centered cubic Al and found that the coefficients are $D_0 = 6.5 \times 10^{-5}$ m^2/s, Q = 136.1 kJ/mol in the temperature range of 859~928 K. Intermetallic phase formation during solid-state diffusion between binary dissimilar metals is an important phenomenon in the Al–Cu welded and bonded components, composites, thin-film electronic devices. Previous study showed that different intermetallic phases may form at the Al–Cu solid-state diffusion interface in terms of the different methods and conditions used in the experiments. Funamizu and Watanabe [3] studied the multiphase diffusion between Cu and Al using bulk couples at 673~808 K for a maximum duration of 100 h. They reported the formation of all the possible five equilibrium phases predicted by the Al–Cu phase diagram, i.e., Al_4Cu_9, Al_2Cu_3, Al_3Cu_4, AlCu, and Al_2Cu. However, Hannech et al. [9] found that the Al_4Cu_9 was absent in the bulk couples annealed at 698 K for 25~225 h. Moreover, in the case of the hot roll bonded Al–Cu laminates, the formation of intermetallic phases was not only dependent on the temperature [10], but also on the time as well [11]. In addition, Abbasi et al. [12] investigated the cold roll bonded Al–Cu bimetal annealed at 523 K for 1~1000 h and detected $AlCu_3$, Al_3Cu_4, AlCu, and Al_2Cu at the interface. However, in the friction-welded Al–Cu bimetallic joints annealed at 573~773 K for 1~36 h, Lee et al. [13] only found two intermetallic phases (AlCu and Al_2Cu) at the interface. As stated above, there are several variables, such as the processing condition, annealing temperature and holding time, that can affect the formation of the intermetallic phases at the interface. However, there is still some scientific confusion about the reactive phase formation between Cu and Al that needs to be clarified. There is a consensus; the kind and amount of the intermetallic phases are the key factors that affect joint properties. So exploring the intermetallic phases generation based on the atomic diffusion in the process of friction welding but not in subsequent annealing process is necessary.

* Corresponding author. Tel.: +86 29 88460673, fax: +86 29 88491426.
E-mail address: lijinglg@nwpu.edu.cn (J. Li).
Peer review under responsibility of Karabuk University.

http://dx.doi.org/10.1016/j.jestch.2015.05.009

This study focuses on the interdiffusion and intermetallic phase formation on Al–Cu interface fabricated by continuous drive friction welding (CDFW). The interfacial morphology and intermetallic phases formed are examined. The sequence of the phase formation is rationalized using the effective heat of formation (EHF) model and thermodynamic analysis. The growth kinetic of the intermetallic layers is determined simultaneously.

2. Experimental procedure

Commercially available bars of Cu (99.9 wt. %) and Al (99.1 wt. %) were used. The specimens were machined with a dimension of 20 mm in welding part and 14 mm in clamping part. Before welding, the welding faces were milled and degreased with acetone. Continuous drive friction welding studies were carried out on a continuous drive friction welding machine of 40 kN capacity at constant friction force (19.1 MPa), forge force (31.8 MPa) and speed of rotation (1900 rpm), and different friction time as 2 s, 4 s, 6 s and 8 s. Friction and upset pressures can be observed on pressure indicator, and the stages of the welding sequence are controlled by solenoid valve driven by an external timer. The surface temperature on the welding joint was observed using an infrared thermographic camera (InfraTec VarioCAM®hr head-HS) at a frame rate of 60 fps. The weld joints were subjected to metallographic characterization employing scanning electron microscopy (SEM) and X-ray diffraction (XRD) technique.

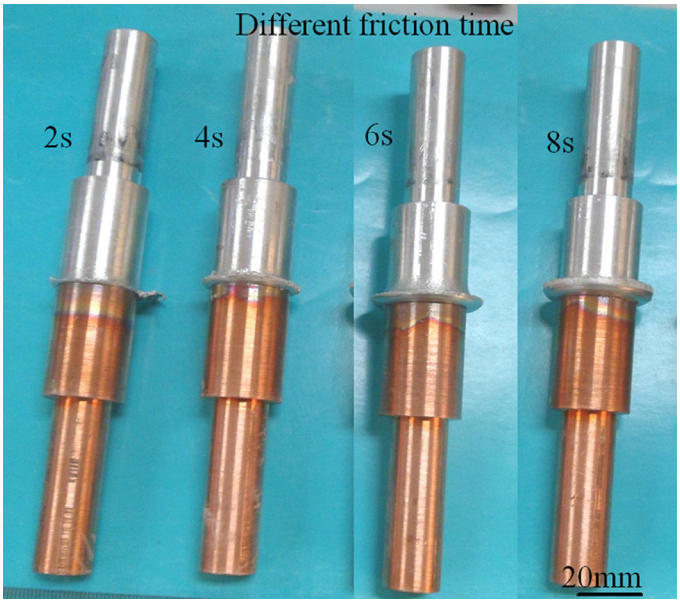

Fig. 1. Macro structures of the welds at different parameters.

3. Results and discussion

3.1. Welding temperature of the plastic region on welding joint

The joints processed by CDFW exhibited good bonding between Al and Cu bars. The samples' appearances are shown in Fig. 1. It can be seen that Al having lower strength experienced more deformation resulting in more flash. The Cu side has no flash produced almost. Moreover, the flash of the Al side significantly increased with the extension of welding time.

The actual temperature of the plastic region on the Al–Cu welding joint is usually an important parameter for the analysis of joint microstructure, interdiffusion, and intermetallic phase formation. In this paper, the temperature of the welding interface region was measured by the infrared thermographic camera during CDFW process of Al–Cu bars, as shown in Fig. 2. Fig. 2a is a typical infrared thermal image of the welding interface region, and Fig. 2b is the variation in the maximum surface temperature of the welding interface region T with different welding time. It can be perceived that the variation of the maximum surface temperature has an unsteady stage and then become more stable, except for the welding time 2 s which is too late to achieve stable stage. The average temperatures processed by the steady stage data were 648 ± 15 K, 665 ± 15 K, 693 ± 15 K and 713 ± 10 K. respectively. Xiong et al. [14] found that the measured average temperature and the maximum temperature of the welding interface region T were lower than, but close to, the welding interface temperature calculated by an analytical model, which was systematically examined by comparing the analytical solutions with corresponding experimental results

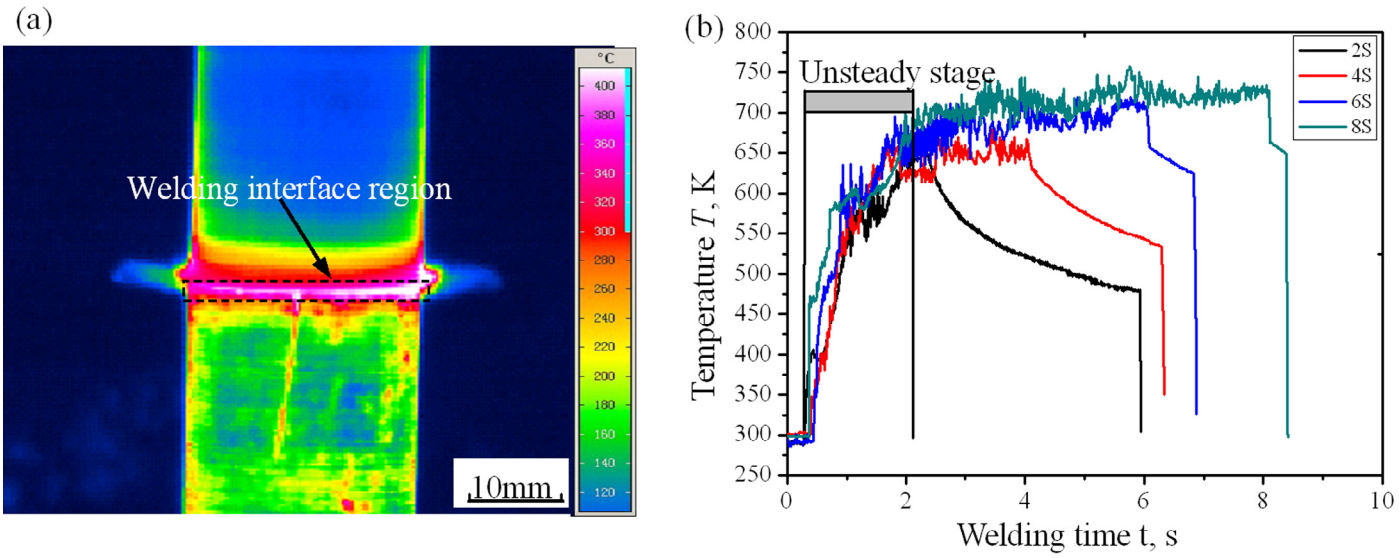

Fig. 2. Actual CDFW process of Al–Cu tubes: (a) The location of the welding interface region in a typical infrared thermal image, and (b) variation in the maximum surface temperature of the welding interface region T with different welding time.

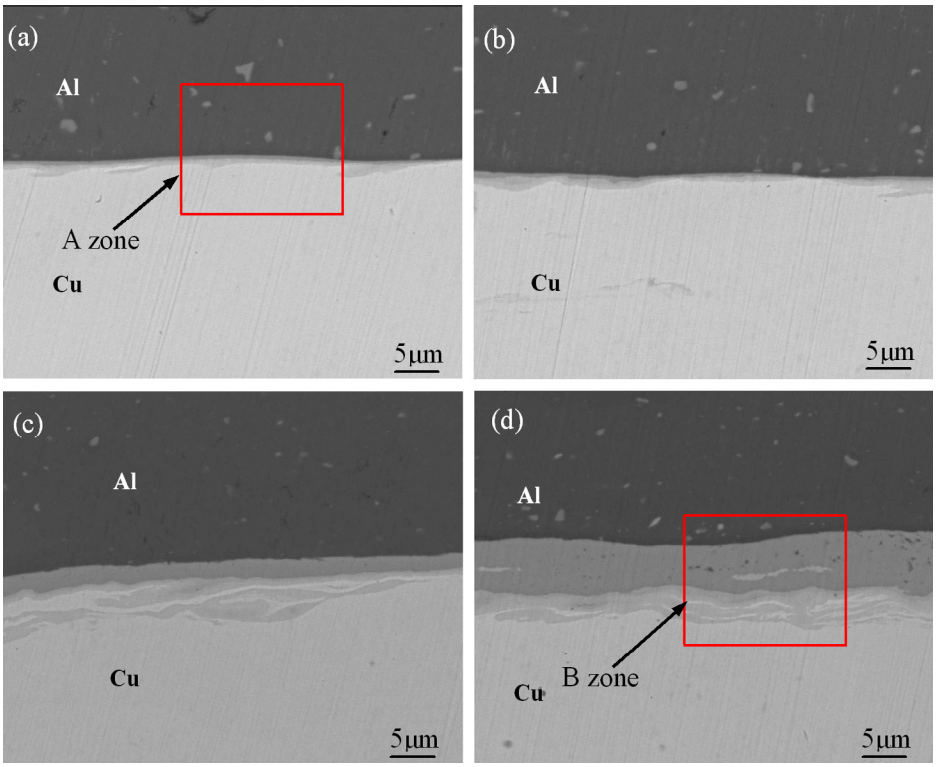

Fig. 3. SEM micrographs of the interfacial regions at friction time: (a) 2 s, (b) 4 s, (c) 6 s and (d) 8 s.

obtained from the CDFW of Al tubes. Therefore, it could be deemed to the actual temperature on the interface.

3.2. *Microstructures and interdiffusion on the joint interface*

Fig. 3 shows the interface microstructures of the Al–Cu joints at different welding parameters. A continuous intermetallic compound layer with a thickness of 0.7 μm~10 μm, parallel to the interface, is distinctly visible between the Al and Cu bulk. The compound layers all consisted of two discernible sub-layer that showed different gray levels at different parameters. The layer closed to Cu side is tortuous and interspersed with Cu matrix. No cracks and voids existed in the interface. The thickness of the IMC layers increased remarkably with the welding time.

High multiple images of the interface region A in Fig. 3a and region B in Fig. 3d are exposed more clearly in Fig. 4. EDS analysis was carried out to investigate the exact composition of IMC layer. Results of EDS analysis conducted on points 1–8 in Fig. 4a and Fig. 4b are then summarized in Table 1. The newly generated layer close to Al side could be identified as Al_2Cu in view of the atom ratio (n(Al):n(Cu)) that is approximately equal to 2:1 in the positions of points 1, 2, 5 and 6. And the layer close to Cu side could be identified as Al_4Cu_9 in view of the atom ratio (n(Al):n(Cu)) that is approximately equal to 4:9 in the positions of points 3, 4, 7 and 8. These phases were further determined by XRD analyses, as shown in Fig. 5. The IMC phases (Al_2Cu, Al_4Cu_9) appeared and were consistent with the above-mentioned EDS analysis.

The interdiffusion between Al and Cu during CDFW process of Al–Cu bars was very obvious. Fig. 6 shows the diffusion layer and the EDS analysis results when the friction time was 8 s. EDS (line canning analysis along the dotted line shown in Fig. 6a) analysis results are shown in Fig. 6b. Linear traces of Al and Cu contents show a relative intensity of Al and Cu. It can be seen that the width of the diffusion layer is about 7.9 μm, which contains two layers of

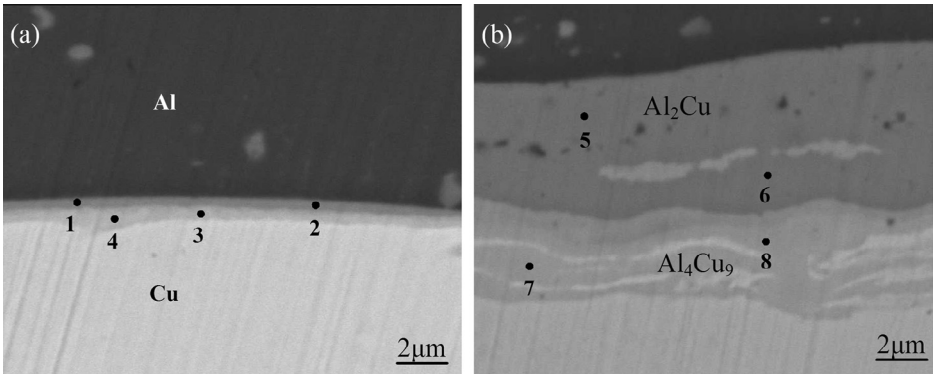

Fig. 4. Micrographs of IMC formed in a state of layer showing (a) enlarged view of zone A in Fig. 3a and (b) enlarged view of zone B in Fig. 3d.

Table 1
Chemical composition of the points indicated in Fig. 4(at.%).

Point	x(Al)/%	x(Cu)/%	n(Al):n(Cu)
1	65.65	34.35	~2:1
2	66.29	33.71	
3	31.87	68.13	~4:9
4	29.71	70.29	
5	67.12	32.88	~2:1
6	64.67	35.33	
7	29.76	70.24	~4:9
8	26.98	73.02	

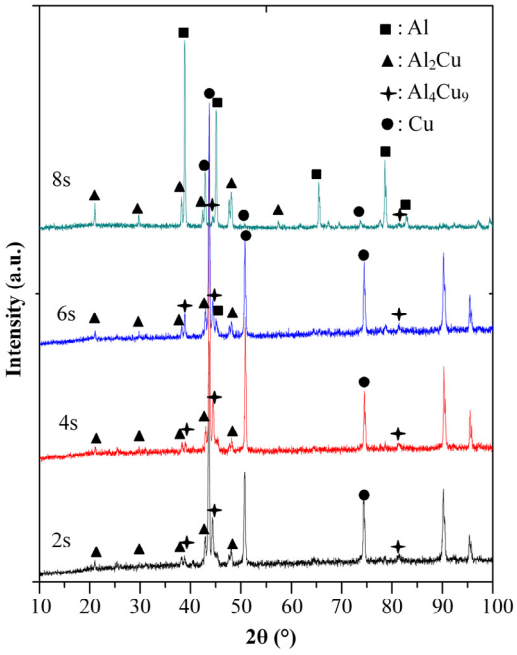

Fig. 5. XRD patterns taken from cross section.

formations. The interdiffusion coefficient can be simply calculated by x^2/t, as 7.8×10^{-12} m^2/s, which is three orders of magnitude compared with diffusion coefficient in literature ($T = 713$ K, $D_0 = 6.5 \times 10^{-5}$ m^2/s, $Q = 136.1$ kJ/mol, so $D = 6.9 \times 10^{-15}$ m^2/s) [8] and is seven orders of magnitude compared with diffusion coefficient under thermal equilibrium state ($T = 713$ K, $D_0 = 1.31 \times 10^{-5}$ m^2/s, $Q = 185.2$ kJ/mol, so $D = 3.5 \times 10^{-19}$ m^2/s) [15]. The interdiffusion between Al and Cu atoms is extraordinarily rapid during the CDFW process of Al–Cu.

3.3. Formation mechanism of interfacial phases of Al–Cu joint

During CDFW, the temperature in the friction interface of Al–Cu joint is in the range of 648~723 K. In this temperature range, the Al–Cu phase diagram indicates that there are five equilibrium phase, Al_2Cu, AlCu, Al_3Cu_4, Al_2Cu_3 and Al_4Cu_9, in the temperature range 623~773 K. In this study, only Al_2Cu and Al_4Cu_9 were found. But other compounds, such as AlCu, Al_3Cu_4, and Al_2Cu_3, should also be formed based on the Al–Cu phase diagram. In general, the sequence of intermetallic phase formation for a binary system is determined not only by the thermodynamics but also the diffusion kinetics.

A number of models were used to predict the formation of first phase in a binary system previously. The effective heat of formation (EHF) model developed by Pretorius et al. [16] was the latest and most effective method used in predicting the formation of first phase in many binary systems (like M–Al) and succeeded in predicting the formation of first phase for 15 metal–Al binary systems. Guo et al. [17] calculated the values of the effective heat of formation, ΔH^e, for all the five intermetallic phases in the temperature range 673~773 K, and found that Al_2Cu has the maximum negative EHF (ΔH^e), which was expected to form first in the diffusion zone in view of thermodynamics combined with kinetic theory.

During the CDFW solid-state interfacial reaction, phase formation on the interface is a nonequilibrium process. It is always found that only one or two compound phase forms at interface, which is unlike equilibrium systems where simultaneous formation of a mixture of phases can lead to the lowest free energy state for the system. In this case, the effective Gibbs free energy change of formation (ΔG_e) replaced with the effective heat of formation (ΔH^e) can more reasonably predict the formation sequence effectively [16]. The

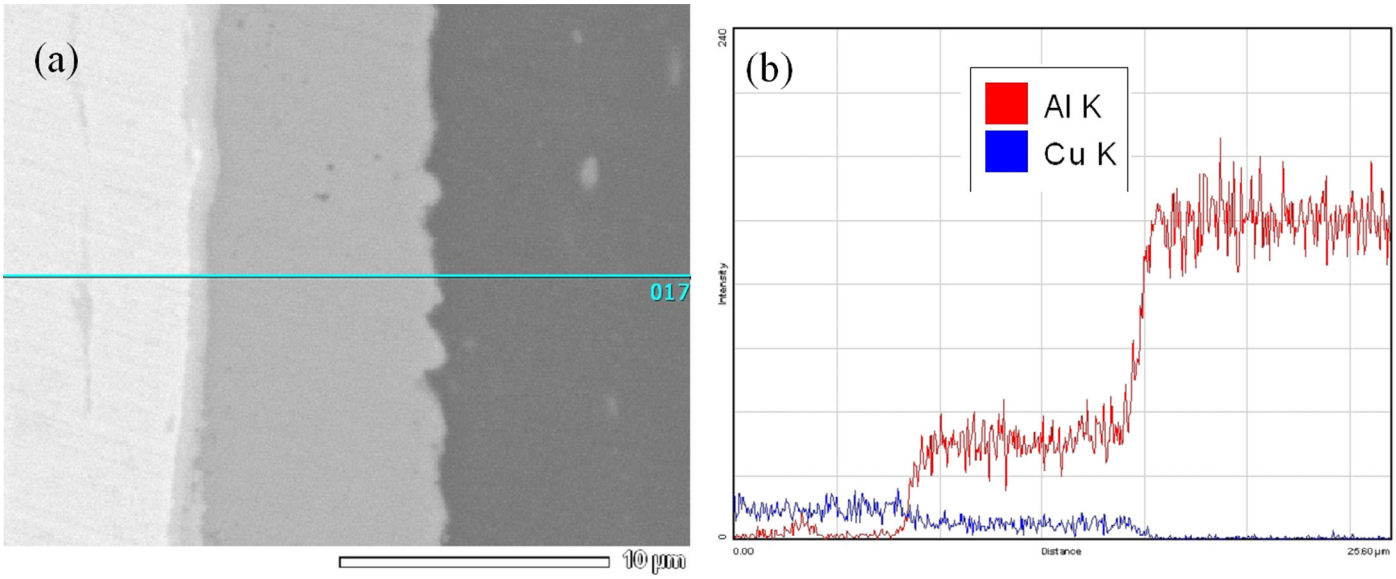

Fig. 6. Qualitative analysis Cu–Al interface shown as (a) SEM image and (b) line scanning results.

Table 2
Gibbs free energy changes of formations (ΔG_{ei}) for Cu–Al compounds at 723K.

Species	Chemical composition	Limiting element	ΔG_i (J/mol) [18]	ΔG_e (723K) (kJ/mol)	ΔG_{ei} (C_e = 0.50) (kJ/mol)
Al_2Cu	$Al_{0.67}Cu_{0.33}$	Al	−15 826.2 + 2.3T	−14.16	−10.57
AlCu	$Al_{0.50}Cu_{0.50}$	Cu(Al)	−20 496.8 + 1.6T	−19.34	−19.34
Al_3Cu_4	$Al_{0.43}Cu_{0.57}$	Cu	−20 197.4 + 1.9T	−18.82	−16.51
Al_2Cu_3	$Al_{0.40}Cu_{0.60}$	Cu	−20 137.8 + 1.6T	−18.98	−15.82
Al_4Cu_9	$Al_{0.31}Cu_{0.69}$	Cu	−19 707.1 + 1.6T	−18.55	−13.44

effective Gibbs free energy change of formation for the i formation phase of Al–Cu interfacial reaction ΔG_{ei}, is defined as:

$$\Delta G_{ei} = \Delta G_i \times \frac{C_e}{C_1} \quad (1)$$

where ΔG_i is the Gibbs free energy change of formation for the i formation phase, C_e the effective concentration of the limiting element at the interface and C_1 the concentration of the limiting element in the compound.

In this study, the interface temperature is deemed to be about 723 K in view of the temperature measurement in section 3.1. For example, if one considers the formation of the phase Al_2Cu at 723 K, and assumes that the effective concentration of Cu at the growth interface is 50 at.% and Al is 50 at.%, Al is therefore the limiting element. The Gibbs free energy change of formation (ΔG_i) for Al_2Cu was −14 160 J/mol, which was calculated by fitting the data of ΔG_i at different temperatures in Yang et al. [18] study. Table 2 shows the calculated results of the effective Gibbs free energy change of formation (ΔG_{ei}) for all Cu aluminide phases at $Al_{0.50}Cu_{0.50}$.

Based on Eq. (1), the effective Gibbs free energy change of formation of any compound for Al–Cu binary system can be calculated as a function of the concentration of the reacting species. Such calculations can be represented graphically, and the effective Gibbs free energy change of formation diagram for the Al–Cu system, as shown in Fig. 7. It can be seen that each phase has the most negative ΔG_{ei}, and thus the release of the most energy from the system occurs when the interfacial actual concentration matches that of a particular phase.

According to Fig. 7, Al_2Cu is expected to be the first phase in the concentration of 0~34.8 at.% of Cu. And Al_4Cu_9 is expected to be the first phase in 59.2~100 at.% and AlCu in 34.8~59.2 at.% accordingly. For the Al–Cu binary system, saturated solid solutions of Al(Cu) and Cu(Al) form on either side due to mutual diffusion. It is to be noted that the solubility limit of Cu in Al is ~0.15 at.% in the temperature range ~723 K, whereas the maximum solubility limit of Al in Cu in the same temperature range is ~18 at.%. Since the solubility limit of Cu in Al is almost two orders of magnitude less than that of Al in Cu, the Al(Cu) solid solution would expect to saturate first. The concentration of Cu must be in the content of 0~34.8 at.%. Therefore, Al_2Cu is the first phase formation at the interface as has been experimentally observed. With the diffusion further, the Cu (Al) solid solution was saturated, and the Al_4Cu_9 phase form at the Cu–Al_2Cu interface. The AlCu phase may appear as the welding time extension. Similar results, showing that the result in Fig. 7 is correct, were found in some other literatures and obtained by other researchers. Saeid et al. [6] and Zhang et al. [19] investigated the friction stir lap joints of Al–Cu and found Al_2Cu and Al_4Cu_9 on the interface. The reaction temperature and time on Al–Cu interface are approximately equivalent. Hang et al. [20] studied the growth behavior of Al–Cu intermetallic compounds in copper ball bonds during isothermal aging, and confirmed that Al_4Cu_9 and Al_2Cu were the main IMC products, while a third phase is found which possibly is CuAl. According to these papers, the Al_2Cu and Al_4Cu_9 were formed first, and the CuAl phase was formed subsequently. It is consistent with the results in Fig. 7.

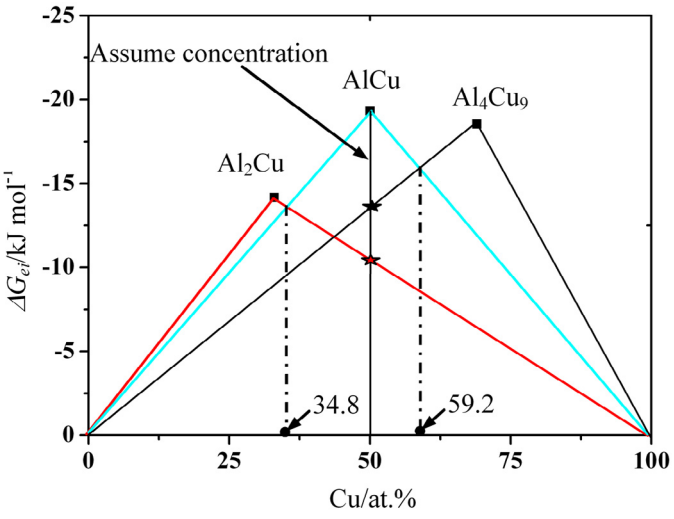

Fig. 7. Effective Gibbs free energy changes of formations (ΔG_{ei}) for Cu–Al compounds under different concentrations.

4. Conclusions

The joints between Al and Cu bars were fabricated by CDFW successfully. The microstructures and the compositions of the composites were analyzed, and the surface temperature was observed. The main conclusions are summarized as follows:

(1) The interface temperatures were suggested in the range of 648~723 K at different welding parameters in view of the measured surface maximum temperature of the welding interface region.
(2) The Al–Cu joints processed by CDFW exhibited defect-free interface. A continuous intermetallic compound layer with a thickness of 0.7 μm~10 μm is distinctly visible, which consisted of two discernible different gray level sub-layers. Intermetallic phases Al_2Cu and Al_4Cu_9 were identified in all samples in view of the XRD and EDS analyses. The interdiffusion coefficient can be simply calculated as 7.8×10^{-12} m^2/s.
(3) The effective Gibbs free energy change of formation model was used to predict the Al–Cu compound formation, and the calculation showed that Al_2Cu (Al side) and Al_4Cu_9 (Cu side) appeared first.

Acknowledgments

This work is financially supported by the fund of the State Key Laboratory of Solidification Processing in NWPU (Grant Nos. 43-QP-2009 and 31-TP-2009) and 111 Project (B08040).

References

[1] J.P. Immarigeon, R.P. Holt, A.K. Koul, L. Zhao, W. Wallace, J.C. Beddoes, Lightweight materials for aircraft applications, Mater. Charact. 35 (1995) 41–67.

[2] J.E. Lee, D.H. Bae, W.S. Chung, K.H. Kim, J.H. Lee, Y.R. Cho, Effects of annealing on the mechanical and interface properties of stainless steel/aluminium/copper clad-metal sheets, J. Mater. Process. Technol. 187–188 (2007) 546–549.
[3] Y. Funamizu, K. Watanabe, Interdiffusion in Al-Cu System, Trans. Jpn. Inst. Met. 12 (3) (1971) 147–152.
[4] J.H. Ouyang, E. Yarrapareddy, R. Kovacevic, Microstructural evolution in the friction stir welded 6061 aluminum alloy (T6-temper condition) to copper, J. Mater. Process. Technol. 172 (2006) 110–122.
[5] A. Abdollah-zadeh, T. Saeid, B. Sazgari, Microstructural and mechanical properties of friction stir welded aluminum/copper lap joints, J. Alloys Compd. 460 (2008) 535–538.
[6] T. Saeid, A. Abdollah-zadeh, B. Sazgari, Weldability and mechanical properties of dissimilar aluminum–copper lap joints made by friction stir welding, J. Alloys Compd. 490 (2010) 652–655.
[7] H.T.G. Hentzell, K.N. Tu, Interdiffusion in copper–aluminum thin film bilayers. II. Analysis of marker motion during sequential compound formation, J. Appl. Phys. 54 (12) (1983) 6929–6937.
[8] Y. Du, Y.A. Chang, B.Y. Huang, W.P. Gong, Z.P. Jin, H.H. Xu, et al., Diffusion coefficients of some solutes in fcc and liquid Al: critical evaluation and correlation, Mater. Sci. Eng. A 363 (2003) 140–151.
[9] E.B. Hannech, N. Lamoudi, N. Benslim, B. Makhloufi, Intermetallic formation in the aluminum–copper system, Surf. Rev. Lett. 10 (2003) 677–683.
[10] X.K. Peng, G. Heness, W.Y. Yeung, Effect of rolling temperature on interface and bond strength development of roll bonded copper/aluminium metal laminates, J. Mater. Sci. 34 (2) (1999) 277–281.
[11] G. Heness, R. Wuhrer, W.Y. Yeung, Interfacial strength development of roll-bonded aluminium/copper metal laminates, Mater. Sci. Eng. A 483 (1–2) (2008) 740–742.
[12] M. Abbasi, A. Karimi Taheri, M.T. Salehi, Growth rate of intermetallic compounds in Al/Cu bimetal produced by cold roll welding process, J. Alloys Compd. 319 (1–2) (2001) 233–241.
[13] W.B. Lee, K.S. Bang, S.B. Jung, Effects of intermetallic compound on the electrical and mechanical properties of friction welded Cu/Al bimetallic joints during annealing, J. Alloys Compd. 390 (1–2) (2005) 212–219.
[14] J.T. Xiong, J.L. Li, Y.N. Wei, F.S. Zhang, W.D. Huang, An analytical model of steady-state continuous drive friction welding, Acta Mater. 61 (2013) 1662–1675.
[15] G. Neumann, C. Tuijn, Self-Diffusion and Impurity Diffusion in Pure Metals: Handbook of Experimental Data, Elsevier, Amsterdam, 2009, pp. 45–54.
[16] R. Pretorius, A.M. Vredenberg, F.W. Saris, Prediction of phase formation sequence and phase stability in binary metal–aluminum thin–film systems using the effective heat of formation rule, J. Appl. Phys. 70 (7) (1991) 3636–3646.
[17] Y.J. Guo, G.W. Liu, H.Y. Jin, Z.Q. Shi, G.J. Qiao, Intermetallic phase formation in diffusion–bonded Cu/Al laminates, J. Mater. Sci. 46 (8) (2010) 2467–2473.
[18] L. Yang, B.X. Mi, L. Lin, H.J. Huang, X.P. Lin, X.G. Yuan, Formation sequence of interface intermetallic phases of cold rolling Cu/Al clad metal sheet in annealing process. China Materials Conference: 23 W material surface and interface, 2012, pp. 1–6.
[19] J.Q. Zhang, Y.F. Shen, X. Yao, H.S. Xu, B. Li, Investigation on dissimilar underwater friction stir lap welding of 6061-T6 aluminum alloy to pure copper, Mater. Des. 64 (2014) 74–80.
[20] C.J. Hang, C.Q. Wang, M. Mayer, Y.H. Tian, Y. Zhou, H.H. Wang, Growth behavior of Cu/Al intermetallic compounds and cracks in copper ball bonds during isothermal aging, Microelectronics Reliability 48 (2008) 416–424.